Received: 23 October 2016 | Accepted: 25 September 2017

DOI: 10.1002/hyp.11371

WILEY

RESEARCH ARTICLE

Hurricanes and tropical storms: A necessary evil to ensure water supply?

Meijing Zhang[1,2] | Xing Chen[1] | Mukesh Kumar[1] | Marco Marani[1] | Michael Goralczyk[1]

[1] Nicholas School of the Environment, Duke University, Durham, NC 27708, USA

[2] Department of Agricultural and Biological Engineering, University of Florida, Homestead, FL 33031, USA

Correspondence
Mukesh Kumar, Nicholas School of the Environment, Duke University, Durham, NC 27708, USA.
Email: mukesh.kumar@duke.edu

Funding information
Hunt Oil Company; National Science Foundation, Grant/Award Numbers: EAR-1331846 and EAR-1454983

Abstract

Several parts of the globe including Southeast North America, the Caribbean, Southeast Asia, Australia, and China are often hit by hurricanes and tropical storms (HTSs), which can deliver a large amount of rainfall within a period of a few days. Although HTSs are mostly studied as disaster agents, considering that they occur during the period when water supply systems are generally depleted, it is important to ascertain their potential contributions toward sustaining water supply. Using the Lake Michie–Little River reservoir system that supplies water to the city of Durham (North Carolina) as a representative test case, we implemented an integrated watershed and reservoir management model, supported by publicly available observations, to evaluate the extent to which HTSs impact water storages. Results indicate that HTSs can have a significant impact on reservoir water storage, with their effects being felt for more than a year for some storms. The impact on reservoir water storage is identified to be primarily controlled by 3 factors, namely, streamflow response size from HTSs, storage in the reservoir right before the event, and streamflow succeeding the event response to HTS (henceforth referred as postevent streamflow). Although the impact of streamflow response size on water storage is generally proportional to its magnitude, initial water storage in the reservoir and postevent streamflow have a nonmonotonic influence on water storage. As all the 3 identified controls are a function of antecedent hydrologic conditions and meteorological forcings, these 2 factors indirectly influence the impact of HTS on water storage in a reservoir. The identification of controlling factors and assessment of their influence on reservoir response will further facilitate implementation of more accurate estimation and prediction frameworks for within-year reservoir operations.

KEYWORDS

distributed hydrologic modelling, drought, hurricanes, reservoir management, tropical storms, water supply

1 | INTRODUCTION

It is estimated that on Earth there are more than 16.7 million reservoirs with a surface area larger than 1×10^{-4} km^2 (Lehner et al., 2011). These reservoirs provide numerous functions, including municipal water supply, irrigation, flood control, hydro-power production, and navigation. Functional efficiency and resiliency of reservoirs, especially the water-supply reservoirs, is crucially dependent on their storage capacity. Larger reservoirs, with volumes much greater than the mean annual cumulative flow, function as "over-year systems"; that is, they are operated according to multiyear regulation schemes (Anderson et al., 2008; Carpenter & Georgakakos, 2001; Graf, 1999; McMahon, Pegram, Vogel, & Peel, 2007; Vogel & Bolognese, 1995; Yao & Georgakakos, 2001). These reservoirs are typical of semiarid regions such as the Southwestern United States and are built to be resilient to seasonal to interannual inflow variability (Graf, 1999; McMahon et al., 2007). In contrast, smaller storage capacity reservoirs generally act as "within-year systems" with discharge and storage rules designed to sustain water demands for a year (Graf, 1999; McMahon et al., 2007). Because of their smaller size, these reservoirs may be vulnerable to seasonal, monthly, and even daily variations in hydrologic inflows and water demands (Hanak & Lund, 2012; Pagano & Garen, 2005; Vogel & Bolognese, 1995; Weaver, 2005). As coastal regions of North and Central America, the Indian subcontinent, Southeast Asia

and Africa, Indo-Malaysia, and Northern Australia are often hit by hurricanes and tropical storms (HTSs; Gray, 1975; Lott & Ross, 2006; Michener, Blood, Bildstein, Brinson, & Gardner, 1997; Powell & Keim, 2015), which can deliver a large amount of rainfall within a period of a few days, a natural question is whether these storms play a significant role in determining within-year reservoir water storage.

Although HTSs have been mostly analysed in terms of their disastrous implications (Ashley & Ashley, 2008; Changnon, 2009; Dale et al., 2001; Elsner, 2007; Emanuel, 1987; Emanuel, Sundararajan, & Williams, 2008; Saunders, Chandler, Merchant, & Roberts, 2000), this study explores their potential positive role in generating water supply. We hypothesize that, especially during times of drought (Chowdhury, 2010; Chu et al., 2002; Golembesky, Sankarasubramanian, & Devineni, 2009; Merabtene, Kawamura, Jinno, & Olsson, 2002; Nakagawa et al., 2000; Wilhite, 1997; Wilhite & Svoboda, 2000), when depleted local water storages have been known to cause severe hardships in municipalities, rain delivered by HTSs may provide a crucial contribution to water supply. Our research goals are to (a) evaluate the extent to which HTSs may impact reservoir water storage, especially in drought years when supply is more vulnerable, and (b) identify the hydrologic controls on HTSs' impact on reservoir storage and assess their individual influences.

2 | DATA AND METHODS

2.1 | Study area and datasets

We use a reservoir system in Southeastern United States, which is often hit by HTSs and droughts (Carter, 1999; White & Wang, 2003), as a representative test case for analyses. One other reason for the selection of this reservoir system is the availability of long-term meteorological, hydrologic, and reservoir management data. The Lake Michie (LM) and Little River (LR) reservoirs (Figure 1) together supply water to the city of Durham, North Carolina. The LM reservoir, which became operational in 1926, drains an area of about 432.8 km^2 and can hold up to 13.63 × 10^6 m^3 of water. The LR reservoir, located to the south of the LM watershed and completed in 1988, drains an area of 260.0 km^2 and has a total storage capacity of 18.68 × 10^6 m^3. The LM and LR active storage volumes, the storage that can be used for water supply, are 10.64 × 10^6 and 13.51 × 10^6 m^3, respectively (Carter, 1999; White & Wang, 2003). The ratio between active reservoir storage volume and annual runoff volume for LM and LR is between 18% and 20%, which is the average storage to runoff ratio for dams in the Northeast and Northwest United States, but lower than the average of 90% in the Southeastern United States (Graf, 1999). The watersheds draining into the LM and LR reservoirs are characterized by valleys oriented in the northwest-to-southeast direction, with elevations ranging from 77 to 270 m above North American Vertical Datum of 1988, according to the 30-m-resolution digital elevation model data from the U.S. Geological Survey (USGS; http://nationalmap.gov/viewer.html; Figure 1b). The watersheds include 15 land cover types based on National Land Cover Data (Fry et al., 2011). The main land cover types are hay or pasture (26.6%), deciduous vegetation (47.2%), developed area (6.9%), and evergreen forest (7.3%; Figure 1c). The study area includes 88 soil types based on Soil Survey Geographic data (Soil Survey Staff, 2013), the majority of the area being loamy soils (Figure 1d). Climate in the study area is characterized by long, hot, humid summers and short, mild winters (Kopec & Clay, 1975). Hourly climate data, including precipitation, temperature, relative humidity, wind velocity, solar radiation, and vapour pressure, were extracted from the North American Land Data

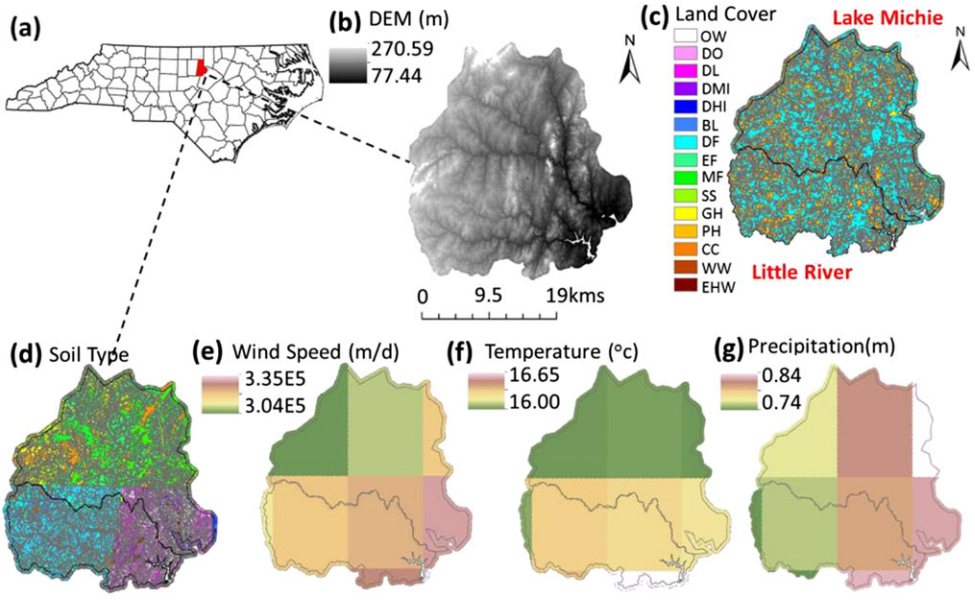

FIGURE 1 (a) North Carolina map, with locations of Lake Michie (LM) and Little River (LR) watersheds identified by red dots. Also shown are the spatial distribution of (b) elevation, (c) land cover, (d) soil cover, (e) average wind speed (year 2007), (f) average temperature (year 2007), and (g) average precipitation (year 2007), in LM and LR watersheds. Land cover abbreviations are as follows: open water (OW); developed, open (DO); developed, low (DL); developed, medium intensity (DMI); developed high intensity (DHI); barren land (BL); deciduous forest (DF); evergreen forest (EF); mixed forest (MF); shrub or scrub (SS); grassland or herbaceous (GH); pasture or hay (PH); cultivated crops (CC); woody wetlands (WW); and emergent herbaceous wetlands (EHW)

Assimilation System phase 2 (NLDAS-2) meteorological forcing dataset (Xia et al., 2012). These forcing data have a spatial resolution of about 9.5 km in the study area (Mitchell et al., 2004; Figure 1e–g).

2.2 | Distributed hydrologic model implementation

The Penn State Integrated Hydrologic Model (PIHM; Kumar, 2009; Qu & Duffy, 2007) was applied to both the LM and LR watersheds to simulate streamflow into the two reservoirs and to evaluate the impact of individual HTSs on water storage in the reservoirs. The model has been previously applied at multiple scales and in diverse hydro-climatological settings for simulating streamflow and coupled hydrologic process dynamics (Chen, Kumar, & McGlynn, 2015; Kumar & Duffy, 2015; Kumar, Marks, Dozier, Reba, & Winstral, 2013; Liu & Kumar, 2016; Seo, Sinha, Mahinthakumar, Sankarasubramanian, & Kumar, 2016; Yu, Duffy, Baldwin, & Lin, 2014). The model uses a physically based, spatially distributed approach to explicitly simulate the coupled surface–subsurface water dynamics and provide estimates of several hydrologic state variables, including surface water depth, soil moisture, groundwater depth, and river stage. A semidiscrete finite volume approach is used to discretize the model domain and define the ordinary differential equations of hydrologic processes on each discretization element. The elements include triangular and linear-shaped units, which represent hillslopes and rivers, respectively. These elements are projected downward to the bedrock to form prismatic and cuboidal elements in 3D. Processes simulated in the model include evaporation, transpiration, infiltration, recharge, overland flow, subsurface flow, and streamflow. Evapotranspiration is computed using the Penman–Monteith method; overland flow is modelled using a diffusion wave approximation to the depth-averaged 2D Saint-Venant equations; subsurface flow modelling is based on Richards' equation using a moving boundary approximation; stream channel routing is modelled with a depth-averaged 1D diffusive wave equation. Vertical infiltration and lateral subsurface flow processes account for the contribution of macropores using a dual-domain approach (Kumar, 2009). The equivalent matrix–macropore system separately considers conductivity and porosity of both macropore and soil matrix to evaluate the flow rates. The model uses an implicit Newton–Krylov integrator, available in the CVODE package (Cohen & Hindmarsh, 1994), to solve for ordinary differential equations in the state variables at each time step. An adaptive time-stepping scheme is used to best capture the process dynamics and optimize the computational burden.

The two watersheds were discretized, horizontally, into a total of 988 land elements and 202 river segments. Vertically, each land element was discretized into four layers: a top overland flow layer, a 0.25-m-thick unsaturated zone, an intermediate unsaturated zone that extends from 0.25-m depth to the water table, and a groundwater layer. Soil moisture in the two unsaturated layers may vary from residual moisture to full saturation. The interface between the two deeper layers moves over time to track the temporally varying groundwater table depth. Each river unit was vertically discretized into two layers, an upper layer to model streamflow and a groundwater zone below it. As the average combined thickness of soil, saprolite, and the transition zone of regolith has been estimated to be less than 20 m in the region (Daniel, 1989), a uniform depth of 20 m was considered as the lower boundary of the subsurface layer. PIHM simulations in the two watersheds were performed for 33 years (1980–2012). The multidecadal simulation period allowed the study of 45 HTSs and of their influence on reservoir water storage. The selected simulation period also provided ample observation data for the validation of simulated streamflow. Hourly streamflow records are available in two major streams within the watershed—at USGS site ID #02085500 on the Flat River at Bahama (point G1 in Figure 2), and at USGS site ID #0208521324 (point G2 in Figure 2) and USGS site ID #02085220 (point G3 in Figure 2) on the LR near Orange Factory. It is to be noted that the PIHM model is used to simulate streamflow and river stage at a total of 202 locations, including five (S1 to S5) that drain into the LM reservoir and seven (G3 and S6 to S11) that drain into the LR reservoir (Figure 2).

2.3 | Reservoir management model implementation

A mass balance scheme is implemented (Figure 2) for both reservoir systems on the basis of

$$S_t = S_{t-1} + P + SF - D - E - O, \tag{1}$$

where S_t and S_{t-1} are the reservoir water storages at time step t and $(t-1)$ respectively; P is the direct precipitation on the reservoir; SF is the streamflow volume input from the watershed into the reservoir; D is the volume of water withdrawn to satisfy water supply requirements; E is the volume evaporated from the reservoir surface; and O is the outflow volume from the reservoir. All volumetric fluxes into and out of the reservoir were evaluated over the time interval $(t-1, t)$. P was extracted from the NLDAS-2 forcing dataset (Xia et al., 2012). The streamflow input into the reservoirs was computed using PIHM simulations at sites S1 to S5, G3, and S6 to S11 (Figure 2). Water demand, D, was measured by the Durham Department of Water Management. As the data for water demand were only available for 1990–2013 (Carter, 1999), daily demand data for 1990, the earliest year with a record, were used for filling the remaining period back to 1980. As the actual water demand is likely to be a bit smaller pre-1990 because of smaller population, this assumption is likely to result in some overestimation in storage deficit. However, consideration of these extra 10 years allowed evaluation of reservoir storage for the entire 33-year simulation period. It is to be noted that the observed demand data quantified the combined water flux withdrawn from the two reservoirs. Withdrawals from each reservoir are estimated on the basis of the current remaining available water storage, according to the following rule:

$$D_{i,t} = D_{\text{total},t}\frac{S_{i,t-1} + SF_{i,t}}{\sum_{i=1}^{2} S_{i,t-1} + SF_{i,t}} \quad (i = 1, 2), \tag{2}$$

where $i = 1$ represents the LM reservoir and $i = 2$ represents the LR reservoir. In reality, day-to-day water quality in the two reservoirs also influenced the decision to withdraw water from a given reservoir, but the overall withdrawal strategy from a reservoir was still based on the need to extract water at a rate proportional to the remaining storage in each reservoir. E was evaluated using meteorological forcings extracted from NLDAS-2 data based on the Penman equation (Penman, 1948). Regression relations between reservoir storage and surface area

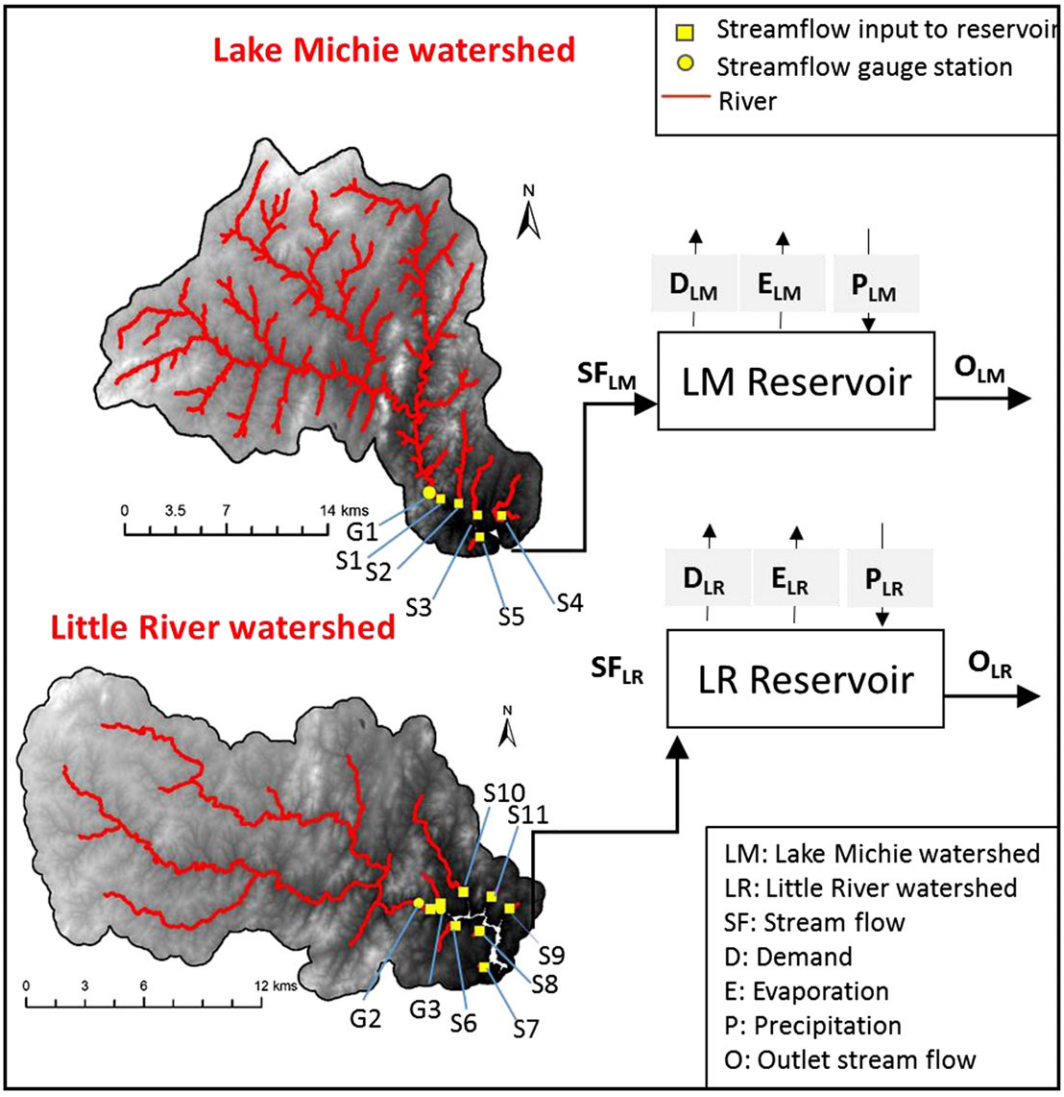

FIGURE 2 Conceptual integration of LM and LR watersheds with drainage reservoirs. Watershed model, Penn State Integrated Hydrologic Model, was implemented in the two watersheds to evaluate streamflow inputs into the reservoir at 12 locations (S1 to S5, G3, and S6 to S11), whereas reservoir management model was implemented to evaluate storage and outflow from the reservoirs

were used to calculate the evaporative surface area of each reservoir (Carter, 1999):

$$\begin{cases} A_{LM} = 0.141\, S_{LM} + 195421.8 \\ A_{LR} = 0.106\, S_{LR} + 292323.5 \end{cases}, \quad (3)$$

where A_{LM} is surface area of the LM reservoir and A_{LR} is surface area of LR reservoir in square metre, whereas storages S_{LM} and S_{LR} are in cubic metres. Outflow from the reservoir, O, was simulated using reservoir rules. For the LM reservoir, the rules mandated the following: (a) The minimum release from the LM reservoir must be 757 m^3/day between November 1 and May 31, and 24.2 m^3/day between July 1 and October 31; and (b) if the reservoir storage is above 70% of the working volume, the minimum release should be 113.4 m^3/day during August, and 87,065 m^3/day during September and October. For the LR reservoir, the outlet discharge used the following prescriptions: (a) Should the reservoir storage ratio drop below 20% of the working volume, the minimum release from the LR reservoir must be 756 m^3/day; (b) should the reservoir storage ratio be above 90% of the working volume, the minimum release from the LR reservoir must be 15,120 m^3/day; and (c) should the reservoir storage ratio be between 20% and 90% of the working volume, the minimum release from the LR reservoir must be 7,560 m^3/day between May 1 and October 31, and 15,120 m^3/day between November 1 and April 30.

2.4 | Model parameterization, calibration, and validation

A geographic information system framework, PIHMgis (Bhatt, Kumar, & Duffy, 2014), was used to automatically parameterize the hydrogeological, ecological, and meteorological properties in the model domain using the datasets described in Section 2.1. In both LM and LR watersheds, PIHM simulations were performed for 33 years (1980–2012). The calibration of model parameters was performed using streamflow data for 2004–2012, which received a mean annual precipitation of 1,080 mm, the same as the average precipitation for the entire simulation period. The calibration process involved nudging

hydrogeological parameters uniformly across the model domain (Refsgaard & Storm, 1996) to match the base flow magnitude and the rate of hydrograph decay during recession. First, a PIHM simulation was conducted by fully saturating the soil to the land surface. The model was then allowed to drain with no precipitation input until streamflow reached an approximately constant value. The simulated hydrograph magnitude at this level state was compared with observed streamflow during late recession periods (5 days after a streamflow peak) in the months of April to July, the period when the streamflow is dominated by base flow in the watershed. Next, the simulated recession rate based on the relaxation hydrograph was compared with the observed recession rates from January to December, when the effect of evapotranspiration is relatively small. The two comparisons yield calibrated hydrogeological properties such as the van Genuchten coefficients in the soil–water retention curves (Van Genuchten, 1980), macro and matrix porosity and conductivity. For reference, the calibration file used for the PIHM simulation is shown in Tables S1 and S2. Modelled and observed water balance statistics during the calibration period (Table 1) indicate a reliable partitioning of the water budget. The model overpredicts the observed annual streamflow by about 16% during the calibration period. The streamflow simulation was compared against observations at sites G1, G2, and G3 (Figure 2) for years 1980–2012 (Figure 3a,b). Gauging station G2 provided observation data for the period January 1, 1980, to September 30, 1987, whereas G3 provided streamflow data for the remaining period until December 22, 2012 (Figure 3b; station G3 was installed in place of G2, which was discontinued on September 30, 1987). Outflow, O, from the two reservoirs were validated at USGS site ID #02086500 located downstream of the reservoir on Flat River and USGS site ID #0208524975 located on the LR at Fairntosh, NC, for the years 2004 to 2012 (Figure 3c,d). Observed and modelled storage ratios, that is, the fraction of combined total water storage in the two reservoirs to the combined storage capacity, for years 2004–2012 were also compared to validate the reservoir management model simulations (Figure 3e). Nash–Sutcliffe efficiency, the coefficient of determination (R^2), root mean square error, Pearson's correlation, and bias of streamflow and reservoir water-storage series (Table 2, Figure 3) show that the coupled hydrologic and reservoir management model was able to effectively quantify the streamflow and reservoir storage time series.

TABLE 1 Key average annual water balance statistics for calibration years (2004–2012)

Watershed	LM	LR
Precipitation (m)	1.083	1.077
Evapotranspiration (m)	0.883	0.89
Observed streamflow (m)	0.193	0.166
Simulated streamflow (m)	0.176	0.156
Observed runoff ratio	0.179	0.154
Simulated runoff ratio	0.163	0.145
RMSE (in m^3/day)	6.29E+05	2.65E+05
Pearson's correlation	0.82	0.86
Bias (%)	−18.33	−15.71

LM = Lake Michie watershed; LR = Little River watersheds; RMSE = root mean square error.

2.5 | Numerical evaluation of the impact of HTSs on reservoir water storage and its theoretical interpretation

The numerical experiment design involved performing individual coupled PIHM and reservoir model simulation (referred to as "scenarios" hereafter) for each of the 33 simulation years (1980–2012). HTS impacts were quantified by evaluating the differences in both modelled streamflow and storage time series in response to precipitation forcings "with HTSs" and "without HTSs." As the impacts of the removal of HTSs on streamflow could potentially last more than a year, each scenario simulation was performed for a 2-year period, starting from the date when the reservoir first falls under 100% capacity (Table 3). For example, the start date for scenarios 19 and 24 (Figure 4) was March 11, 2004, and June 10, 2010, respectively. HTSs were only removed from the precipitation series during the first year of the simulation as the goal was to isolate the impact on streamflow hydrograph if HTSs did not occur in a particular year. Notably, the antecedent hydrologic conditions used in the scenario experiments were identical to those in the 33-year long-term simulation. As 7 out of 33 simulation years did not receive any HTS precipitation and a 2-year simulation (starting from when reservoirs first fall below capacity) could not be performed for the last 2 years in the dataset (2011 and 2012), the total number of scenario simulations was limited to 24. During these 24 years (i.e. the first years in the 2-year scenario simulations), the LM and LR watersheds were hit by 42 large HTSs (Table 3), with total annual event rainfall accumulations between 48 and 152 mm. An HTS event was defined to begin at the start of precipitation and to end when no rainfall has been observed for at least 6 hr. Using the scenario simulation results, the streamflow response size corresponding to HTSs in a given year (column 7 in Table 3) was defined as the difference between the streamflow hydrograph obtained using the without HTSs scenario and that based on the with HTSs long-term simulation. It is to be noted that the difference between two streamflow hydrographs spanned well beyond the duration of an HTS. For example, in scenarios 21 and 24 (Figure 4), duration of the HTS was 4 and 6 days, respectively, whereas the two streamflow hydrographs were appreciably different (difference larger than 10% of the without HTSs case) for around 160 and 182 days. In fact, the difference in the two hydrographs continued through multiple precipitation events following the HTS. This is because the antecedent hydrologic conditions, such as soil moisture and groundwater, for the subsequent storms were different between with HTS and without HTS cases.

The impact of HTSs on reservoir storage was quantified using storage deficit change ($\Delta S_{\text{deficit}}$). First, the storage deficit, S_{deficit}, is defined as the average deficit ratio between $t = 0$ and $t = t_D$:

$$S_{\text{deficit}} = \frac{\int_0^{t_D} (1 - S_{\text{ratio}})\,dt}{t_D}, \tag{4}$$

$$S_{\text{ratio}} = \frac{S_{\text{LM}} + S_{\text{LR}}}{S_{\text{capacity}}}, \tag{5}$$

where $t = 0$ represents the time when the storage ratio first falls below 1, t_D is the time period for which S_{deficit} is evaluated (equal to 1 or 2 years, see discussion below), S_{ratio} is the total storage ratio of both

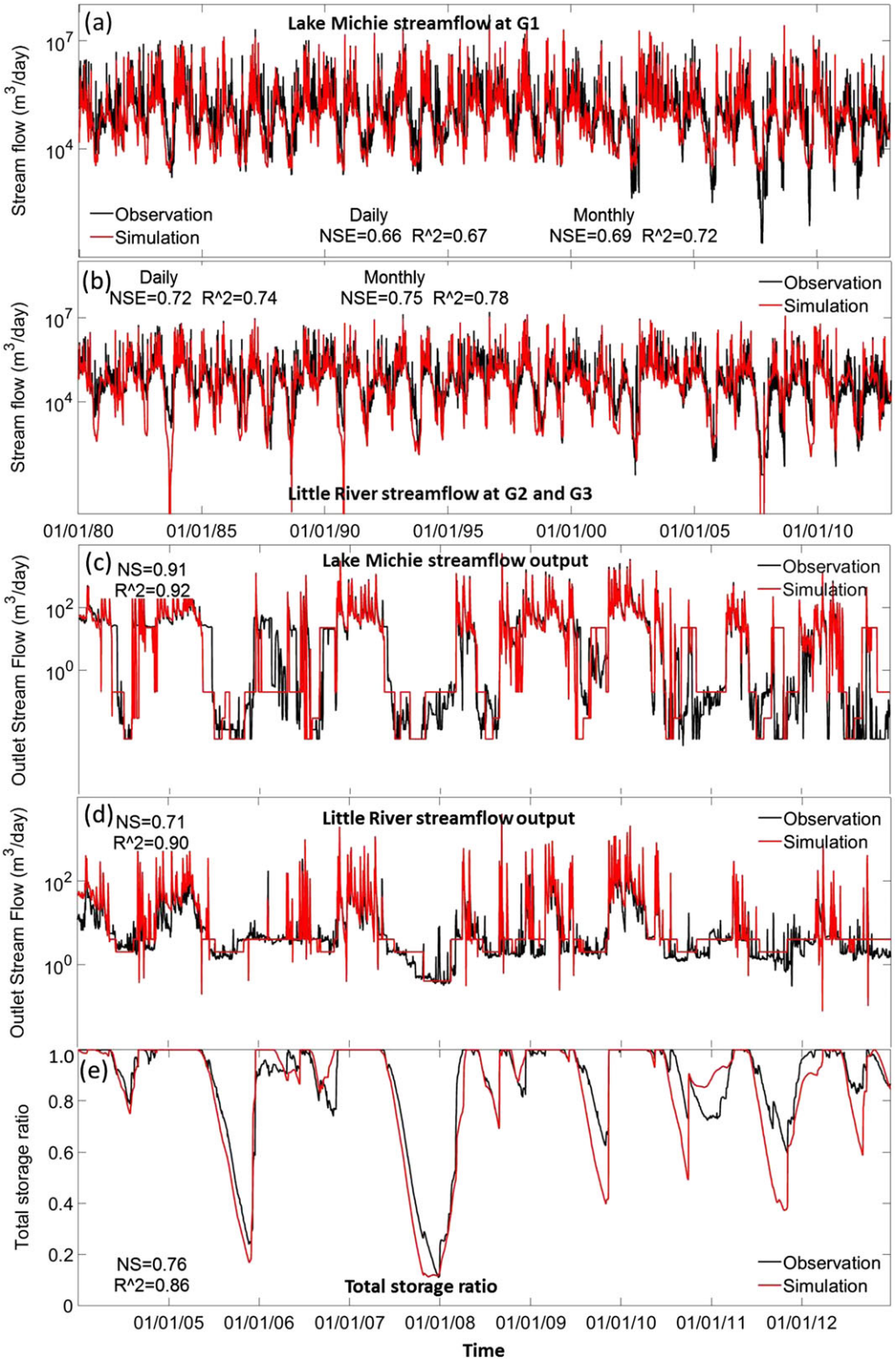

FIGURE 3 Comparison of modelled and observed (a) streamflow at station G1 in Lake Michie (LM) watershed, (b) streamflow at G2 and G3 in the Little River (LR) watershed, (c) outlet streamflow from LM reservoir, (d) outlet streamflow from LR reservoir, and (e) total reservoir storage ratio. NSE = Nash–Sutcliffe efficiency

LM and LR reservoirs, and $S_{capacity}$ is the total storage capacity of the LM and LR reservoirs. An $S_{deficit}$ value of 1.0 indicates that the reservoir was empty for the entire scenario period, whereas a zero $S_{deficit}$ results from a full storage for the entire scenario period. The storage deficit change ($\Delta S_{deficit}$) associated with HTSs for a given scenario is calculated as (Figure 5)

$$\Delta S_{deficit} = S_{deficit}|_{w} - S_{deficit}|_{wt}, \quad (6)$$

TABLE 2 NSE and R^2 for the simulation years (1980–2012)

	SF_LM	SF_LR	O_LM	O_LR	Total S
Daily NSE	0.66	0.72	0.91	0.71	0.76
Daily R^2	.67	.74	.92	.9	.86
Monthly NSE	0.69	0.75	—	—	—
Monthly R^2	.72	.78	—	—	—

LM = Lake Michie reservoir; LR = Little River reservoir; NSE = Nash–Sutcliffe efficiency; O = outflow from the reservoir; SF = streamflow input to the reservoir; Total S = total storage in the two reservoirs.

where $S_{\text{deficit}}|_{\text{w}}$ and $S_{\text{deficit}}|_{\text{wt}}$ are the storage deficits with and without HTSs, respectively. $\Delta S_{\text{deficit}}$ was evaluated for both t_{D} equal to 1 and 2 years. It is to be noted that changes in storage deficit are also accompanied by changes in storage deficit duration (S_{duration}), which is defined as the total number of days (Figure 5) during which the reservoir storage ratio is less than 1 between $t = 0$ and $t = t_{\text{D}}$. The storage deficit duration change ($\Delta S_{\text{duration}}$) is calculated as

$$\Delta S_{\text{duration}} = S_{\text{duration}}|_{\text{wt}} - S_{\text{duration}}|_{\text{w}}, \tag{7}$$

TABLE 3 The 45 largest hurricanes and tropical storms in North Carolina during 1980–2012

Scenario ID	Scenario start	Event name	Event start date	Event end date	Event size (m)	Streamflow response size (m)
1	7/6/1980	TS: Bret	6/30/1981	7/6/1981	0.116	0.027
2	6/14/1983	H: Tico	10/22/1983	10/26/1983	0.048	0.025
3	8/20/1984	TS: Isidore	9/27/1984	10/2/1984	0.052	0.018
4	4/3/1985	TS: Juan TS: Kate	10/30/1985 11/20/1985	11/5/1985 11/23/1985	0.109 0.104	0.147
5	4/6/1986	H: Charley	8/16/1986	8/22/1986	0.093	0.023
6	5/28/1987	TD: Nine	9/3/1987	9/8/1987	0.098	0.023
7	3/26/1988	TD: Chris TS: Isaac	8/28/1988 10/2/1988	8/31/1988 10/4/1988	0.068 0.061	0.030
8	6/29/1989	TS: Barry	7/15/1989	7/18/1989	0.052	0.013
9	6/13/1990	H: Klaus H: Lili	10/10/1990 10/21/1990	10/13/1990 10/24/1990	0.099 0.083	0.085
10	6/3/1991	TS: Ana	9/24/1991	9/26/1991	0.077	0.028
11	5/12/1994	TD: Two	7/25/1994	7/29/1994	0.063	0.008
12	4/4/1995	H: Allison TD: Jerry H: Opal TS: Sebastien	6/9/1995 8/25/1995 10/3/1995 10/20/1995	6/13/1995 8/28/1995 10/6/1995 10/21/1995	0.052 0.066 0.075 0.053	0.095
13	6/12/1996	H: Fran	9/3/1996	9/7/1996	0.145	0.081
14	6/17/1997	H: Danny H: Erika	7/22/1997 9/9/1997	7/25/1997 9/11/1997	0.058 0.062	0.026
15	6/6/1998	H: Earl	9/3/1998	9/4/1998	0.069	0.015
16	5/11/1999	H: Dennis H: Dennis H: Floyd TS: Harvey	8/25/1999 9/4/1999 9/14/1999 9/26/1999	8/27/1999 9/7/1999 9/16/1999 9/30/1999	0.055 0.152 0.117 0.104	0.237
17	4/20/2001	TS: Gustav TS: Kyle	8/25/2002 10/10/2002	9/3/2002 10/12/2002	0.114 0.141	0.135
18	7/1/2003	TD: Bill H: Isabel H: Juan	7/1/2003 9/18/2003 9/22/2003	7/3/2003 9/19/2003 9/23/2003	0.055 0.056 0.053	0.060
19	3/10/2004	TS: Bonnie TD: Gaston	8/13/2004 8/29/2004	8/17/2004 8/31/2004	0.064 0.061	0.043
20	3/1/2006	TS: Alberto TS: Ernesto H: Isaac	6/13/2006 8/30/2006 10/5/2006	6/14/2006 9/1/2006 10/7/2006	0.053 0.074 0.051	0.058
21	5/1/2007	H: Noel	10/24/2007	10/27/2007	0.102	0.027
22	6/1/2008	H: Gustav H: Hanna	8/25/2008 9/5/2008	8/28/2008 9/6/2008	0.132 0.125	0.121
23	4/27/2009	TD: One H: Ida	6/4/2009 11/10/2009	6/5/2009 11/14/2009	0.070 0.139	0.130
24	6/9/2010	H: Igor	9/26/2010	10/1/2010	0.142	0.041
—	5/18/2011	H: Irene	9/5/2011	9/7/2011	0.064	0.012
—	6/1/2012	TS: Debby H: Sandy	7/9/2012 9/17/2012	7/11/2012 9/19/2012	0.057 0.063	0.106

Each scenario represents a 2-year simulation experiment. Definitions of TS, TD, and H are available at http://www.nhc.noaa.gov/aboutgloss.shtml. H = hurricane; TD = tropical depression; TS = tropical storm.

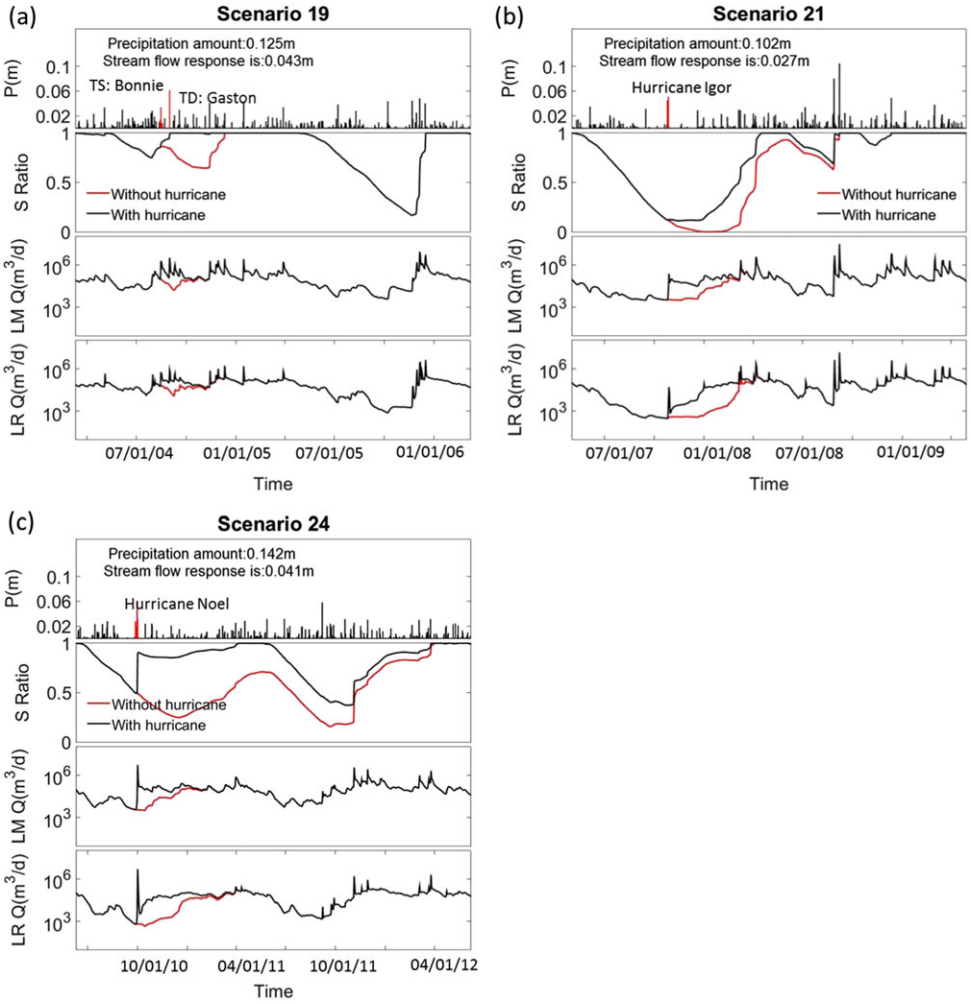

FIGURE 4 Response of reservoir storage ratio and Lake Michie (LM) and Little River (LR) streamflow to hurricanes and tropical storms in (a) scenario 19, (b) scenario 21, and (c) scenario 24. TD = tropical depression; TS = tropical storm

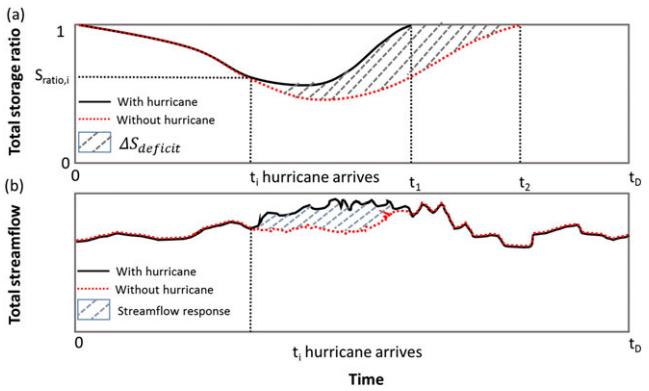

FIGURE 5 (a) Storage deficit change and (b) streamflow response introduced by hurricanes and tropical storms

where $S_{\text{duration}}|_{\text{w}}$ and $S_{\text{duration}}|_{\text{wt}}$ are the storage durations with and without HTSs, respectively. By applying Equations 4 and 6 to the illustrative case depicted in Figure 5, we obtain

$$\Delta S_{\text{deficit}} = \frac{\int_0^{t_2}\left(1-S_{\text{ratio},t}|_{\text{w}}\right)\text{d}t}{t_{\text{D}}} - \frac{\int_0^{t_1}\left(1-S_{\text{ratio},t}|_{\text{wt}}\right)\text{d}t}{t_{\text{D}}}, \tag{8}$$

where $S_{\text{ratio},t}|_{\text{wt}}$ is the total storage ratio at time t for the case without HTSs and $S_{\text{ratio},t}|_{\text{w}}$ is the total storage ratio with HTSs. Given that $S_{\text{ratio},t}|_{\text{w}}$ and $S_{\text{ratio},t}|_{\text{wt}}$ start diverging at time t_i, when the first HTS occurs during the simulation period, the total storage ratio at time $t > t_i$ can be written as

$$S_{\text{ratio},t} = S_{\text{ratio},t_i} + \int_{t_i}^{t}\frac{R}{S_{\text{capacity}}}\text{d}\varsigma, \tag{9}$$

where S_{ratio,t_i} is the total storage ratio at time t_i (Figure 5) and R is the net recharge into the reservoirs at time t, defined as $R = P + SF - D - E - O$. Substituting Equation 9 into Equation 8 yields

$$\Delta S_{\text{deficit}} = \frac{(t_2-t_1)\left(1-S_{\text{ratio},t_i}\right)}{t_{\text{D}}} - \frac{\int_{t_i}^{t_2}\int_{t_i}^{t}R_{\text{w}}\text{d}\varsigma\text{d}t}{t_{\text{D}}} + \frac{\int_{t_i}^{t_1}\int_{t_i}^{t}R_{\text{wt}}\text{d}\varsigma\text{d}t}{t_{\text{D}}}. \tag{10}$$

According to Equation 10, the difference in deficit with and without HTSs can be attributed to the differences in the initial reservoir storage conditions (S_{ratio,t_i}), ($t_2 - t_1$), and to the difference in recharge rate, R, since time t_i. We note that ($t_2 - t_1$) indirectly depends on the initial storage conditions and on R in the reservoirs with and without hurricanes. Hence, the initial storage and the reservoir recharge rate can be considered as the primary controls on the difference in

storage deficit. As the recharge rate, R, is a function of P, SF, D, E, and O (see definitions of variables used in Equation 9), the difference in any of these variables after an HTS can lead to a difference in storage deficit change.

3 | RESULTS AND DISCUSSION

3.1 | Role of HTSs on storage in water-supply reservoirs

Comparisons of $S_{deficit}$ and deficit durations for the 24 scenario experiments listed in Table 3 show that storage deficit and durations increase markedly when HTSs are removed (Table 4). Results show that the average $S_{deficit}$ increases from 0.15 to 0.20 for t_D = 2 years and from 0.15 to 0.24 for t_D = 1 year, if contributions from HTSs are removed. The average of relative change in storage deficit, that is, $\Delta S_{deficit}/S_{deficit|w}$, was 41% and 113% for t_D = 2 and 1 year, respectively. Notably, $\Delta S_{deficit}$ for t_D = 1 year is larger than that for t_D = 2 years because the influence of HTSs on storage deficit for the majority of scenarios lasted less than a year. $\Delta S_{deficit}$ varied markedly across scenarios. For example, $\Delta S_{deficit}$ was zero for scenarios 1 and 17 for t_D = 1 year (Table 4). In contrast, for years 1999 (scenario 16) and 2010 (scenario 24), $\Delta S_{deficit}$ was as large as 0.35 (relative change of 438%) and 0.33 (relative change of 275%), respectively, for t_D = 1 year. The average deficit duration also changed appreciably, increasing from 240 to 287 days for t_D = 1 year and from 350 to 402 days for t_D = 2 years when HTSs were removed. The average of relative change in deficit duration was 24% and 17% for t_D = 1 and 2 years, respectively. The largest deficit duration change during the simulation period was 192 days (Table 4) for 1999 (scenario 16). According to the 2-year scenario simulations, the duration for which the combined reservoir water storage was below 25% of its capacity, the storage level below which water conservation ordinances are issued, increased from 179 to 458 days (relative change of 156%) when the influence of HTSs was not considered. The time it takes for the reservoir to be full again (t_1 and t_2 in Figure 5) also increased from 207 to 291 days when the influence of HTSs was not accounted for. For some years, for example, 1985 (scenario 4), ($t_2 - t_1$) was longer than a year (Table 4). A comparison of reservoir storage ratio for with and without HTSs cases showed a statistically significant difference between the two cases, on the basis of a two-sample Kolmogorov–Smirnov test with a p value of .05. For 1-year scenario simulations, the minimum S_{ratio} value was 0.11 and 0 for with and without HTSs cases (Figure 6), respectively. The fraction of time that the reservoir was full reduced from 34.6% to 21.9% when impact of HTSs was ignored. For the 2-year scenario simulations, the reservoir was full for 37.5% and 30.4% of the time for with and without HTS cases, respectively. These results suggest

TABLE 4 Variation of storage deficit and storage deficit duration obtained from 24 scenario experiments

	t_D = 1 year			t_D = 2 years			t_D = 1 year			t_D = 2 years			t_D = 2 years
ID	SDw	SDwt	SDC	SDw	SDwt	SDC	SDDw (days)	SDDwt (days)	SDDC (days)	SDDw (days)	SDDwt (days)	SDDC (days)	$t_2 - t_1$ (days)
1	0.21	0.21	0.00	0.13	0.21	0.08	365	365	0	576	585	9	9
2	0.15	0.16	0.01	0.13	0.14	0.01	186	192	6	437	443	6	6
3	0.15	0.18	0.03	0.12	0.14	0.01	276	304	28	491	519	28	28
4	0.09	0.17	0.08	0.14	0.21	0.07	219	366	147	484	639	155	424
5	0.19	0.27	0.08	0.18	0.22	0.04	266	287	21	356	377	21	21
6	0.18	0.24	0.07	0.18	0.21	0.03	294	324	30	390	420	30	30
7	0.19	0.31	0.12	0.10	0.16	0.06	333	343	10	413	423	10	10
8	0.01	0.03	0.02	0.06	0.06	0.01	111	111	0	125	125	0	0
9	0.10	0.24	0.14	0.15	0.22	0.07	167	234	67	284	351	67	67
10	0.20	0.25	0.05	0.14	0.17	0.03	235	292	57	343	400	57	57
11	0.26	0.31	0.04	0.16	0.18	0.02	319	320	1	369	370	1	1
12	0.06	0.14	0.08	0.05	0.09	0.04	189	280	91	189	280	91	6
13	0.03	0.09	0.05	0.08	0.11	0.03	112	202	90	188	278	90	90
14	0.13	0.21	0.07	0.21	0.24	0.04	213	228	15	246	261	15	15
15	0.28	0.33	0.05	0.18	0.21	0.02	262	264	2	349	351	2	2
16	0.08	0.43	0.35	0.17	0.35	0.17	161	353	192	264	456	192	235
17	0.33	0.33	0.00	0.31	0.38	0.07	365	365	0	550	626	76	76
18	0.02	0.07	0.06	0.03	0.06	0.03	233	286	53	232	285	53	0
19	0.04	0.12	0.08	0.15	0.18	0.04	190	275	85	297	382	85	100
20	0.04	0.09	0.05	0.26	0.28	0.03	216	249	33	257	290	33	21
21	0.51	0.62	0.11	0.28	0.35	0.07	350	366	16	457	505	48	144
22	0.05	0.20	0.15	0.09	0.17	0.08	195	265	70	259	329	70	131
23	0.13	0.21	0.08	0.13	0.17	0.04	189	240	51	209	260	51	192
24	0.12	0.45	0.33	0.18	0.41	0.23	323	366	43	641	691	50	362

$t_2 - t_1$ is shown in Figure 5. HTSs = hurricanes and tropical storms; SDC = $S_{deficit}$ change ($\Delta S_{deficit}$); SDDC = $S_{deficit}$ duration change ($\Delta S_{duration}$); SDDw = $S_{deficit}$ duration with HTSs ($S_{duration|w}$); SDDwt = $S_{deficit}$ duration without HTSs ($S_{duration|wt}$); SDw = $S_{deficit}$ with HTSs ($S_{deficit|w}$); SDwt = $S_{deficit}$ without HTSs ($S_{deficit|wt}$).

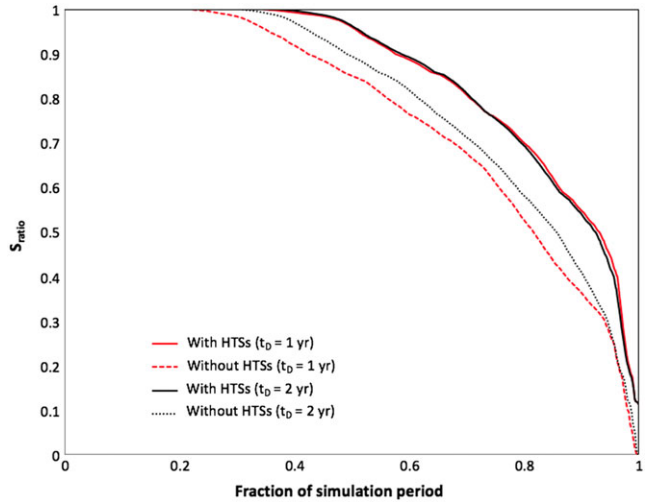

FIGURE 6 Fraction of scenario simulation period for which the reservoir storage is larger than the corresponding value on the *y* axis for with and without hurricanes and tropical storms (HTSs) cases

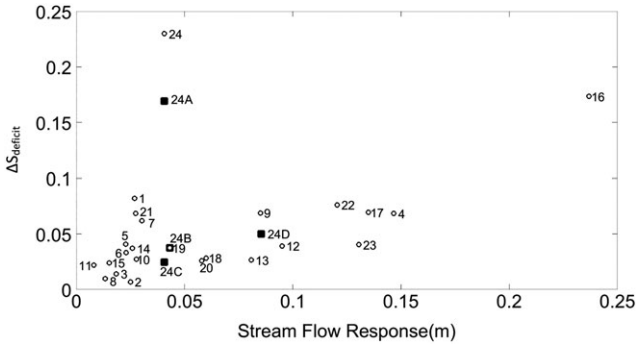

FIGURE 7 Variation of storage deficit change with streamflow response. Numbers in the plot represent scenario IDs defined in Table 3. Scenario 24A is performed using the same forcing as in scenario 24, but the initial reservoir storage ratio is set identical to that in scenario 19; scenario 24B is performed using the same forcings as in scenario 24A, but the initial reservoir storage ratio and postevent streamflow are the same as for scenario 19; configuration of scenario 24C is the same as that of scenario 24, except that the initial reservoir storage ratio is set identical to that in scenario 19 and the postevent streamflow ratio is 1.5; configuration of scenario 24D is the same as that of scenario 24, except that the initial reservoir storage ratio, antecedent soil moisture, and groundwater conditions are set identical to those in scenario 19

that HTSs may have a very significant impact on both storage deficit amount and duration, with evident and important implications. For example, in December 2007, levels in Durham's reservoirs were so low that only 1 month's worth of water remained in storage (Greeley, 2015). Our simulations (scenario 21 in Table 3) show that, were it not for Hurricane Noel, which delivered around 0.102 m of precipitation in the area, the water storage in LM and LR reservoirs would have gone below the operational volume limit (Figure 4b). Although the streamflow response volume to Hurricane Noel was only around 0.027 m, this amount was sufficient to avoid complete depletion of the two reservoirs. In the absence of this event and of any water conservation measures, the time for which the reservoir was below 25% of its working volume would have increased from 93 to 141 days. In fact, in absence of HTS events, the reservoir was likely to be below its working volume for 17 days in 2007, with $\Delta S_{duration}$ being 48 days. The influence of Hurricane Noel was large enough to last more than 144 days, influencing storage deficit in 2008 too.

3.2 | Controls on the storage deficit change in water-supply reservoirs

The main difference between with HTSs and without HTSs cases is the streamflow input to the reservoir, which is expected to be the primary determinant of $\Delta S_{deficit}$. Figure 7 shows that the storage deficit changes induced by HTSs are on average proportional to the streamflow response size. Spearman's rank correlation between $\Delta S_{deficit}$ and streamflow response size is 0.60, confirming that the streamflow amount generated by HTSs indeed influences the $\Delta S_{deficit}$ magnitude to a large degree. It is to be noted, however, that there are multiple pairs of scenarios, for example, scenarios 4 and 23, 2 and 21, 19 and 24, for which $\Delta S_{deficit}$ were markedly different even when the streamflow response magnitude was similar (Figure 7). To understand the cause of variations in $\Delta S_{deficit}$ to similarly sized streamflow responses, we select scenarios 19 and 24 for further analyses.

In scenario 19, tropical storms Bonnie and Gaston delivered about 0.125 m of precipitation, which led to a streamflow response of 0.043 m and a $\Delta S_{deficit}$ of 0.037 and $\Delta S_{duration}$ of 85 days (Figure 4a). HTS-caused streamflow response in scenario 24 was almost identical to the streamflow response in scenario 19 (Figure 7). In this case, Hurricane Igor delivered 0.142 m of precipitation, which led to a streamflow response of 0.041 m. Notably, $\Delta S_{deficit}$ for scenario 24 was equal to 0.230, which is much larger than that of scenario 19. As discussed in Section 2.5, the difference in $\Delta S_{deficit}$ between the two scenarios is attributable to the differences in the initial reservoir storage conditions (S_{ratio,t_i}) and in the recharge rate *R*, which, in turn, is a function of *P*, *SF*, *D*, *E*, and *O* (see Equations 9 and 10). To isolate the role of initial storage condition, the reservoir model was rerun for scenario 24 by setting the initial storage to be equal to that of scenario 19. For the new simulation (scenario 24A), the storage deficit change declined from 0.23 to 0.169, still a much larger value than $\Delta S_{deficit}$= 0.037 for scenario 19 (Figure 7). This suggests that the initial storage in the reservoirs only partially explains the difference in $\Delta S_{deficit}$ between the two scenarios. Next, the reservoir model for scenario 24A was rerun by artificially setting the recharge rate *R* to be identical to that of scenario 19. As would be expected on the basis of Equation 10, the value of $\Delta S_{deficit}$ for this scenario (scenario 24B) was exactly equal to that for scenario 19. The result suggests that although S_{ratio,t_i} plays an important role in determining the difference in $\Delta S_{deficit}$ between scenarios 19 and 24, its contribution is relatively minor with respect to that of *R*. As the recharge rate, *R*, is a function of *P*, *SF*, *D*, *E*, and *O* (see Equation 9), we next evaluate the role of *SF*, the primary driver of variation in $\Delta S_{deficit}$. Because the event streamflow response for both the scenarios were almost identical, we directly evaluated the role of streamflow following the event response to HTS. We call this the postevent streamflow. Total postevent *SF* for LM and LR reservoirs was 0.39 and 0.35 m for scenario 19, and 0.26 and 0.25 m for scenario 24, respectively. This indicates that, on average, postevent

streamflow during scenario 19 was approximately 1.5 times larger than that in scenario 24. Next, a new scenario simulation was performed (scenario 24C) by setting the postevent *SF* of scenario 24A to be 1.5 times its magnitude. Results show that storage deficit change was reduced (from 0.23 in scenario 24) to 0.025, which is very close to $\Delta S_{deficit}$ of 0.037 that occurred in scenario 19 (Figure 7). This highlights that initial reservoir storage and postevent *SF* played a major role in the variable reservoir storage response between scenarios 19 and 24. It is to be noted that postevent streamflow between the two scenarios can be different due to a host of factors, including antecedent hydrologic states and meteorological forcings. In fact, the hydrologic states of the two watersheds right before the hurricane events in the two scenarios were markedly different. For example, in scenario 19, average antecedent effective soil saturation (defined as [absolute moisture content-residual porosity]/[saturated moisture content-residual porosity]) within the top 25 cm of the land surface in the LM and LR watersheds were 0.26 and 0.25, respectively. In scenario 24, the top soil was extremely dry with spatially averaged effective saturation of about 0.002. The average groundwater depth in scenario 19 in the LM and LR watersheds was 6.9 and 6.4 m, respectively. Corresponding depths in scenario 24 were 18.2 and 12.7 m. To explore the influence of antecedent hydrologic conditions on storage deficit change, one additional simulation (scenario 24D) was run on the basis of scenario 24A, by setting the antecedent soil and groundwater conditions to those of scenario 19. Results show that storage deficit change in scenario 24D decreased to 0.050 (Figure 7), close to the $\Delta S_{deficit}$ of 0.037 for scenario 19. This means that antecedent subsurface conditions played a substantial role in determining the difference in postevent *SF* and storage deficit change between scenarios 19 and 24. By setting the meteorological forcings in scenario 24D to be the same as those of scenario 19, $\Delta S_{deficit}$ becomes identical to that of scenario 19.

In summary, the above analysis indicates that the variations in $\Delta S_{deficit}$ are fundamentally impacted by the magnitude of the streamflow response to HTSs. Events generating larger streamflow response are mostly associated with larger $\Delta S_{deficit}$. Initial reservoir storage and postevent streamflow, which in turn is a function of antecedent hydrologic conditions and meteorological forcings, may also markedly influence the magnitude of $\Delta S_{deficit}$. It is to be highlighted that the streamflow response size to HTSs is itself influenced by precipitation characteristics such as volume and duration, antecedent hydrologic conditions, and meteorological conditions immediately following the events (Castillo, Gomez-Plaza, & Martınez-Mena, 2003; Chen et al., 2015; Tramblay et al., 2010). Other participating factors such as municipal demand rates, and evapotranspiration play a minor role on variations in $\Delta S_{deficit}$. In fact, changes in average demand and evapotranspiration between with and without HTS cases were only 0.06 and 0.53 mm, respectively, while the average *SF* change was 56 mm.

3.3 | Role of initial reservoir storage ratio and postevent streamflow on variable reservoir storage response

The analysis in Section 3.2 confirmed that in addition to streamflow response size, the initial reservoir storage and postevent *SF* may markedly influence the variation in $\Delta S_{deficit}$. We now analyse in greater detail the magnitude and sign of this influence on $\Delta S_{deficit}$. To this end, nine additional pairs of reservoir simulations were run for each of the 24 scenario experiments. The paired simulations were designed to capture the influence of HTSs on reservoir water storage deficit for a range of initial reservoir storage and postevent streamflow. To understand the variation of $\Delta S_{deficit}$ in relation to the initial reservoir storage ($S_{ratio,i}$), reservoir simulations were performed by setting the initial reservoirs storage ratios to 10%, 20%, …, 90% of their total operational capacities, whereas other model configurations remained the same as those described in Section 2.5. The results (Figure 8a) suggest that in 13 out of 24 scenarios, $\Delta S_{deficit}$ showed a monotonic decreasing trend (e.g., for scenario 19) as S_{ratio,t_i} increased, whereas in the remaining cases (e.g., for scenario 24), $\Delta S_{deficit}$ exhibited a slight initial increase, before decreasing at larger values of S_{ratio,t_i}. The reason for the decreasing trend in $\Delta S_{deficit}$ is evident from the comparison of reservoir storage time series with and without HTSs for a range of initial reservoir storages in

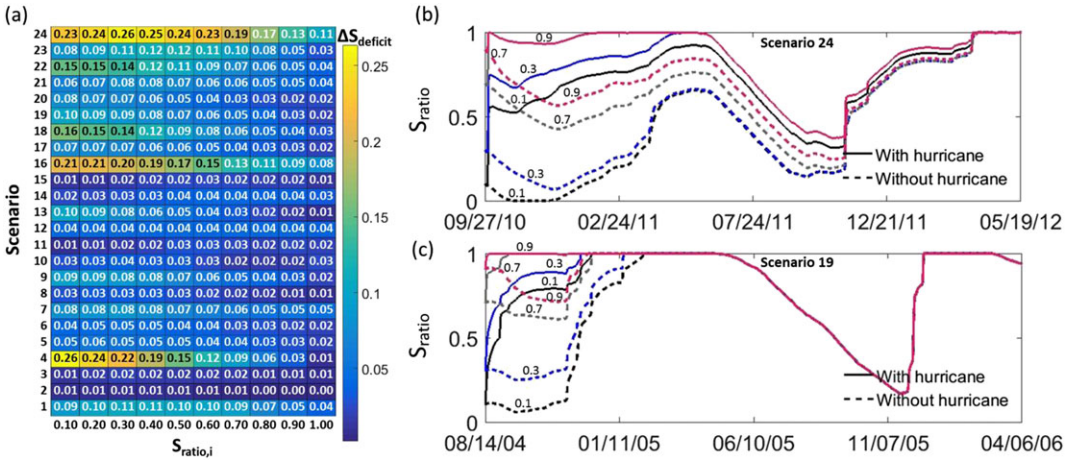

FIGURE 8 (a) Influence of initial reservoir storage conditions on change in storage deficit ($\Delta S_{deficit}$) due to hurricanes and tropical storms for the 24 scenarios listed in Table 3. Numbers indicate the magnitude of $\Delta S_{deficit}$; (b) reservoir storage deficit time series for scenario 24; and (c) reservoir storage deficit time series for scenario 19. In (b) and (c), colours identify different initial reservoir storage ratios

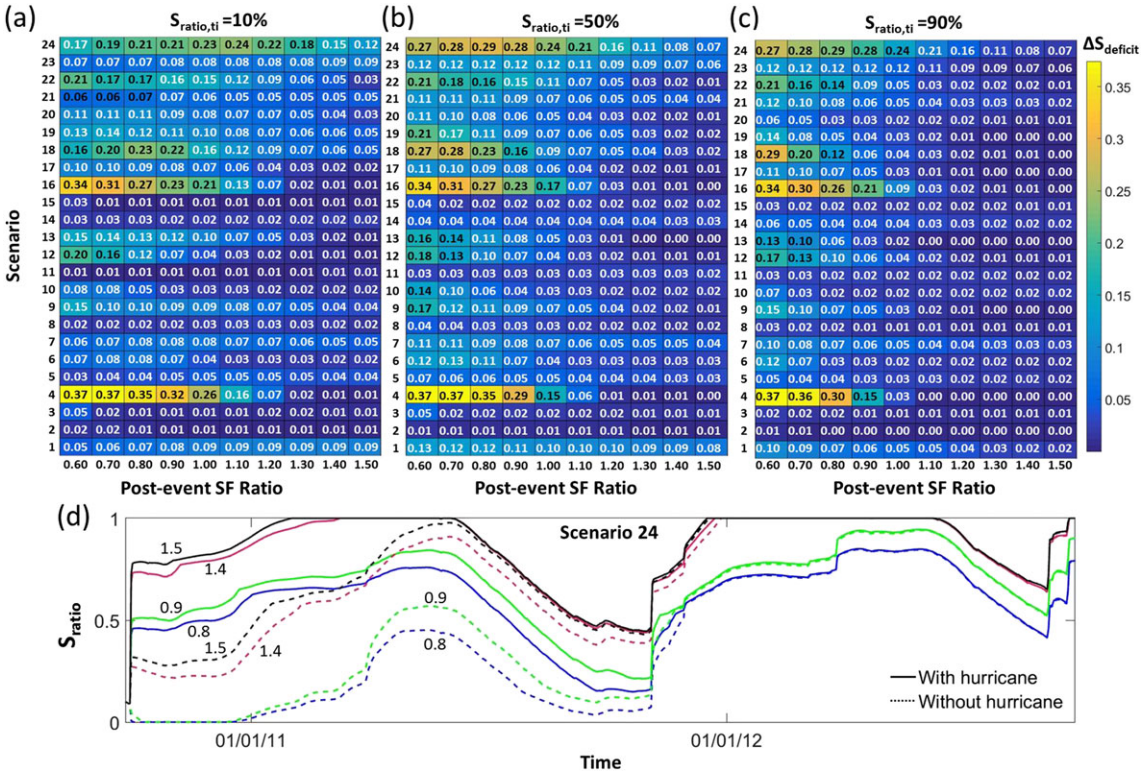

FIGURE 9 Influence of postevent streamflow on the change in storage deficit ($\Delta S_{deficit}$) due to hurricanes and tropical storms for the 24 scenarios listed in Table 3, when (a) initial storage ratio is 10%, (b) initial storage ratio is 50%, and (c) initial storage ratio is 90%; (d) storage ratio time series for scenario 24 with initial storage ratio of 10%. Numbers in (a)–(c) indicate the magnitude of $\Delta S_{deficit}$. Colours in (d) identify different ratios of postevent streamflow

Figure 8c. As S_{ratio,t_i} increases, so is the increase in both $S_{ratio,t}|_w$ and $S_{ratio,t}|_{wt}$. However, for larger values of S_{ratio,t_i} (e.g., $S_{ratio,\,i}$ equal to 0.7 or 0.9 in Figure 8c), $S_{ratio,t}|_w$ is equal to its ceiling value of 1 for a longer period and, hence, does not increase as much as $S_{ratio,t}|_{wt}$. As a result, $\Delta S_{deficit}$ decreases with increasing S_{ratio,t_i}. For the scenarios exhibiting a nonmonotonic trend (e.g., scenario 24 in Figure 8a and 8b), $\Delta S_{deficit}$ still increases with decrease in S_{ratio,t_i} until a certain threshold value of S_{ratio,t_i} is reached. For example, the threshold S_{ratio,t_i} for scenario 24 is 0.3. However, below this threshold, $\Delta S_{deficit}$ decreases with a decrease in S_{ratio,t_i}. The reason for this reversal in the trend of $\Delta S_{deficit}$ is evident from the comparison of reservoir storage time series in Figure 8b. For smaller values of S_{ratio,t_i} (e.g., $S_{ratio,\,i}$ equal to 0.1 in Figure 8b), $S_{ratio,t}|_{wt}$ becomes zero, indicating that the reservoir level has fallen below its operating capacity when the HTSs are removed. With a further decrease in S_{ratio,t_i}, $S_{ratio,t}|_{wt}$ is equal to zero for a longer period of time, and hence, $S_{ratio,t}|_{wt}$ does not decrease as much as $S_{ratio,t}|_w$. As a result, $\Delta S_{deficit}$ decreases with decrease in initial reservoir ratio below a certain S_{ratio,t_i} threshold, thereby resulting in a nonmonotonic trend in $\Delta S_{deficit}$. Notably, even for the 11 scenarios for which $\Delta S_{deficit}$ showed a nonmonotonic trend, $\Delta S_{deficit}$ for ($S_{ratio,\,i}$ = 0.1) was on an average 55% larger than its value at ($S_{ratio,\,i}$ = 1) was. For 12 out of 13 scenarios for which $\Delta S_{deficit}$ decreased monotonically with increase in $S_{ratio,\,i}$, $\Delta S_{deficit}$ for $S_{ratio,\,i}$ = 0.1 was on an average 485% larger than its value at $S_{ratio,\,i}$ = 1 was. These results indicate that for a given HTS, the impact on storage deficit is generally larger if it happened during a period with the smallest $S_{ratio,\,i}$. For the 33-year simulation period, the $S_{ratio,\,i}$ was generally the smallest during September, thus indicating the HTSs in September may generally have a large influence on storage deficit.

To investigate the variation in $\Delta S_{deficit}$ vis-à-vis postevent *SF* magnitude, nine reservoir simulations were performed for each of the 24 scenarios by setting the postevent streamflow *SF* to be 0.6, 0.7, ..., 1.4, 1.5 times the *SF* from the reference simulation. The remaining model configurations, such as the HTS-generated streamflow response, initial reservoir storage ratios, and meteorological forcings, remained the same. The relationship between the storage deficit change and the postevent *SF* is shown in Figure 9a–c, for S_{ratio,t_i} equal to 10%, 50%, and 90% of total storage capacity, respectively. $\Delta S_{deficit}$ again decreased with increasing postevent streamflow in some scenarios and showed an initial increase followed by a subsequent decline in others. The expressed trends can again be explained on the basis of the logic presented earlier. For relatively large postevent *SF*, the likelihood of $S_{ratio,t}|_w$ to be equal to 1 increases, thus limiting its rate of increase with postevent *SF*. This results in a decrease in $\Delta S_{deficit}$ with increase in postevent *SF*. However, below a threshold postevent *SF* magnitude, $\Delta S_{deficit}$ decreases with postevent *SF* as the reservoir is likely to be empty for a longer time if HTSs are removed, such that $S_{ratio,t}|_{wt}$ does not decrease as much as $S_{ratio,t}|_w$ (Figure 9d).

4 | SUMMARY AND CONCLUSIONS

An integrated watershed and reservoir management model, in the same vein as one presented by Zhao, Gao, Naz, Kao, and Voisin

(2016), was implemented to investigate the extent to which HTSs may impact storage deficit in a within-year water-supply reservoir. The integrated model was designed to simulate streamflow input to the reservoirs, streamflow output from the reservoirs, and reservoir storage time series. The distributed nature of the model allowed simulation of streamflow time series at 12 input locations into the reservoirs. The validated model was subsequently used to evaluate the differences in simulated (streamflow and reservoir storage) response when forced by precipitation series with HTSs and without HTSs. The model was then also used to identify the controlling factors that led to differences in hydrologic response between with and without HTS cases. The process-explicit nature of the model allowed isolating the influences of each control by one by one changing its magnitude while leaving the initial conditions of other state variables unchanged.

This study shows that even though HTSs are isolated annual events, they can produce long-term effects over interannual time scales. Model results demonstrate that the simulated streamflow response and consequent storage deficit in the reservoir were appreciably different between with HTSs and without HTSs cases, with differences in response spanning well beyond the duration of HTSs. The average change in storage deficit between the two cases was 113% and 41% for t_D = 1 and 2 years, respectively, where t_D represents the time since the storage ratio first fell below 1. The average deficit duration also registered appreciable changes, as it increased from 240 to 287 days for t_D = 1 year and from 350 to 402 days for t_D = 2 years when HTSs were removed. The results highlight that water storage in the studied within-year water-supply reservoirs is significantly influenced by precipitation delivered during HTSs. This means that reservoir operations designed to mitigate droughts in these systems can crucially benefit from near-term event-based forecasts. On the flip side, the results indicate that uncertainties in event intensity of projected precipitation events, quite significant and common (Woldemeskel, Sharma, Sivakumar, & Mehrotra, 2012; Xie & Arkin, 1997), may cause large inaccuracies in reservoir storage estimates. Notably, seasonal forecasts of meteorological forcings or streamflow, which are often used for management of over-year reservoirs (Chiew, Zhou, & McMahon, 2003; Li, Xu, Chen, & Simonovic, 2010; Mahanama, Livneh, Koster, Lettenmaier, & Reichle, 2012; Souza Filho & Lall, 2003), may not accurately capture the storage deficit response to HTSs in within-year reservoirs.

Streamflow response size from HTSs, initial reservoir storage ($S_{ratio,\,i}$), and postevent streamflow were identified as the three primary controls on the extent of impact of HTSs on reservoir storage deficit change ($\Delta S_{deficit}$). Overall, the variations in $\Delta S_{deficit}$ were proportional to the streamflow response size to HTSs. However, significant deviations from this rule were observed, in part because of the influence of other two controls. $\Delta S_{deficit}$ was generally smaller for scenarios with larger initial reservoir storage and postevent streamflow magnitude. However, the individual variation of $\Delta S_{deficit}$ vis-à-vis either of these two variables were found to be non-monotonic. For cases when the reservoir level would fall below the operational capacity after the influence of HTSs on storage capacity is discarded, $\Delta S_{deficit}$ showed an opposite trend in variation and instead increased with increasing initial reservoir storage and postevent streamflow magnitude. Notably, even for the scenarios for which $\Delta S_{deficit}$ showed a nonmonotonic trend, $\Delta S_{deficit}$ for $S_{ratio,\,i}$ = 0.1 was on an average 55% larger than its value at $S_{ratio,\,i}$ = 1. This indicates that for a given HTS, the impact on storage deficit is generally larger if it happened during a period with the smallest $S_{ratio,\,i}$. For the 33-year simulation period, the $S_{ratio,\,i}$ was generally the smallest during September, thus indicating that the HTSs in September may generally have a large influence on storage deficit. It is to be noted that all three aforementioned controls are a function of several other transient controls such as antecedent hydrologic conditions, precipitation characteristics, and meteorological conditions; and hence, these factors also indirectly end up affecting the influence of HTSs on reservoir storage deficit. The interdependence found in our analyses between antecedent conditions and HTS effects on water storage is not a trivial one. This underscores the need to appropriately consider variations in event-scale antecedent hydrologic conditions, to obtain a realistic assessment of impacts on storage dynamics in within-year reservoirs. Other influencing factors on $\Delta S_{deficit}$ include municipal demand rates, evapotranspiration, and outflow from the reservoir, but their role was shown to be much smaller in the case of the LM and LR reservoir systems.

The study demonstrates the important role of HTSs on the sustainability of water supply for within-year reservoirs in Southeastern United States. The results are also applicable for other cyclone-prone regions such as the Caribbean, Southeast Asia, China, and Northern Australia. Considering that HTSs are predicted to be more intense over the next century (Easterling, Evans, Groisman, & Karl, 2000; Li, Li, Fu, Deng, & Wang, 2011; Webster, Holland, Curry, & Chang, 2005) and although this trend poses an increased risk to society, we should also recognize and be able to exploit its benefits for water resources availability. The implemented modelling framework may be used to evaluate new reservoir management strategies in a more extreme HTS regime. The framework may also be used to evaluate risks associated with drought and overtopping of reservoirs, due to more extreme precipitation regimes. Future work should focus on evaluating the applicability of these findings to other within-year reservoirs, especially those with markedly different reservoir sizes, and fed by streams with significantly different runoff ratio and relative contribution of groundwater to streamflow during hurricane season. Incidence of HTS would also have implications on reservoir safety particularly when a high volume of flow enters in an already full reservoir; however, our research is not about reservoir safety, but the framework presented in this paper if combined with dam break flood analysis may be used for safety evaluation.

ACKNOWLEDGMENTS

This study was partially supported by the National Science Foundation grants (EAR-1331846 and EAR-1454983) and the Hunt Oil Company. We thank Tom Lucas and Vicki Westbrook of Durham city water supply, treatment, and management services, for providing data regarding reservoir rules.

ORCID

Meijing Zhang http://orcid.org/0000-0001-9550-5498

REFERENCES

Anderson, J., Chung, F., Anderson, M., Brekke, L., Easton, D., Ejeta, M., … Snyder, R. (2008). Progress on incorporating climate change into management of California's water resources. *Climatic Change*, *87*, 91–108.

Ashley, S. T., & Ashley, W. S. (2008). Flood fatalities in the United States. *Journal of Applied Meteorology and Climatology*, *47*, 805–818.

Bhatt, G., Kumar, M., & Duffy, C. J. (2014). A tightly coupled GIS and distributed hydrologic modeling framework. *Environmental Modelling & Software*, *62*, 70–84.

Carpenter, T. M., & Georgakakos, K. P. (2001). Assessment of Folsom lake response to historical and potential future climate scenarios: 1. Forecasting. *Journal of Hydrology*, *249*, 148–175.

Carter, S. (1999). A risk-based simulation model for drought management in Durham, North Carolina. University of North Carolina at Chapel Hill.

Castillo, V., Gomez-Plaza, A., & Martınez-Mena, M. (2003). The role of antecedent soil water content in the runoff response of semiarid catchments: A simulation approach. *Journal of Hydrology*, *284*, 114–130.

Changnon, S. A. (2009). Characteristics of severe Atlantic hurricanes in the United States: 1949–2006. *Natural Hazards*, *48*, 329–337.

Chen, X., Kumar, M., & McGlynn, B. L. (2015). Variations in streamflow response to large hurricane-season storms in a Southeastern US watershed. *Journal of Hydrometeorology*, *16*, 55–69.

Chiew, F., Zhou, S., & McMahon, T. (2003). Use of seasonal streamflow forecasts in water resources management. *Journal of Hydrology*, *270*, 135–144.

Chowdhury, N. T. (2010). Water management in Bangladesh: An analytical review. *Water Policy*, *12*, 32–51.

Chu, G., Liu, J., Sun, Q., Lu, H., Gu, Z., Wang, W., & Liu, T. (2002). The 'mediaeval warm period' drought recorded in Lake Huguangyan, tropical South China. *The Holocene*, *12*, 511–516.

Cohen, S. D., & Hindmarsh, A. C. (1994). CVODE user guide. Technical Report UCRL-MA-118618, LLNL.

Dale, V. H., Joyce, L. A., McNulty, S., Neilson, R. P., Ayres, M. P., Flannigan, M. D., … Peterson, C. J. (2001). Climate change and forest disturbances: Climate change can affect forests by altering the frequency, intensity, duration, and timing of fire, drought, introduced species, insect and pathogen outbreaks, hurricanes, windstorms, ice storms, or landslides. *Bioscience*, *51*, 723–734.

Daniel, C. C. (1989). Statistical analysis relating well yield to construction practices and siting of wells in the Piedmont and Blue Ridge Provinces of North Carolina. USGPO; for sale by the books and open-file reports section, US Geological Survey.

Easterling, D. R., Evans, J., Groisman, P. Y., & Karl, T. (2000). Observed variability and trends in extreme climate events: A brief review. *Bulletin of the American Meteorological Society*, *81*, 417.

Elsner, J. B. (2007). Granger causality and Atlantic hurricanes. *Tellus A*, *59*, 476–485.

Emanuel, K., Sundararajan, R., & Williams, J. (2008). Hurricanes and global warming: Results from downscaling IPCC AR4 simulations. *Bulletin of the American Meteorological Society*, *89*, 347–367.

Emanuel, K. A. (1987). The dependence of hurricane intensity on climate. *Nature*, *326*, 483–485.

Fry, J. A., Xian, G., Jin, S., Dewitz, J. A., Homer, C. G., Limin, Y., … Wickham, J. D. (2011). Completion of the 2006 national land cover database for the conterminous United States. *Photogrammetric Engineering and Remote Sensing*, *77*, 858–864.

Golembesky, K., Sankarasubramanian, A., & Devineni, N. (2009). Improved drought management of Falls Lake Reservoir: Role of multimodel streamflow forecasts in setting up restrictions. *Journal of Water Resources Planning and Management*, *135*, 188–197.

Graf, W. L. (1999). Dam nation: A geographic census of American dams and their large-scale hydrologic impacts. *Water Resources Research*, *35*, 1305–1311.

Gray, W. M. (1975). Tropical cyclone genesis in the western North Pacific. DTIC Document.

Greeley, D. (2015). Running out of water is not an option. https://wrri.ncsu.edu/docs/events/ac2015/GreeleyDon.pdf. Accessed on July 2018, 2016.

Hanak, E., & Lund, J. R. (2012). Adapting California's water management to climate change. *Climatic Change*, *111*, 17–44.

Kopec, R. J., & Clay, J. W. (1975). Climate and air quality. North Carolina atlas—Portrait of a changing southern State, 92–111.

Kumar, M. (2009). Toward a hydrologic modeling system. The Pennsylvania State University, Ann Arbor, p. 274.

Kumar, M., & Duffy, C. (2015). Exploring the role of domain partitioning on efficiency of parallel distributed hydrologic model simulations. *Journal of Hydrogeology & Hydrologic Engineering*, *4*, 1. https://doi.org/10.4172/2325-9647.1000119

Kumar, M., Marks, D., Dozier, J., Reba, M., & Winstral, A. (2013). Evaluation of distributed hydrologic impacts of temperature-index and energy-based snow models. *Advances in Water Resources*, *56*, 77–89.

Lehner, B., Liermann, C. R., Revenga, C., Vörösmarty, C., Fekete, B., Crouzet, P., … Magome, J. (2011). High-resolution mapping of the world's reservoirs and dams for sustainable river-flow management. *Frontiers in Ecology and the Environment*, *9*, 494–502.

Li, L., Xu, H., Chen, X., & Simonovic, S. (2010). Streamflow forecast and reservoir operation performance assessment under climate change. *Water Resources Management*, *24*, 83–104.

Li, W., Li, L., Fu, R., Deng, Y., & Wang, H. (2011). Changes to the North Atlantic subtropical high and its role in the intensification of summer rainfall variability in the Southeastern United States. *Journal of Climate*, *24*, 1499–1506.

Liu, Y., & Kumar, M. (2016). Role of meteorological controls on interannual variations in wet-period characteristics of wetlands. *Water Resources Research*.

Lott, N., & Ross, T. (2006). Tracking and evaluating U.S. billion dollar weather disasters, 1980–2005. Preprints, AMS Forum: Environmental Risk and Impacts on Society: Success and Challenges, Atlanta, GA, Amer. Meteor. Soc., 1.2. [Available online at http://ams.confex.com/ams/Annual2006/techprogram/paper_100686.htm].

Mahanama, S., Livneh, B., Koster, R., Lettenmaier, D., & Reichle, R. (2012). Soil moisture, snow, and seasonal streamflow forecasts in the United States. *Journal of Hydrometeorology*, *13*, 189–203.

McMahon, T. A., Pegram, G. G., Vogel, R. M., & Peel, M. C. (2007). Revisiting reservoir storage–yield relationships using a global streamflow database. *Advances in Water Resources*, *30*, 1858–1872.

Merabtene, T., Kawamura, A., Jinno, K., & Olsson, J. (2002). Risk assessment for optimal drought management of an integrated water resources system using a genetic algorithm. *Hydrological Processes*, *16*, 2189–2208.

Michener, W. K., Blood, E. R., Bildstein, K. L., Brinson, M. M., & Gardner, L. R. (1997). Climate change, hurricanes and tropical storms, and rising sea level in coastal wetlands. *Ecological Applications*, *7*, 770–801.

Mitchell, K. E., Lohmann, D., Houser, P. R., Wood, E. F., Schaake, J. C., Robock, A., … Luo, L. (2004). The multi-institution North American Land Data Assimilation System (NLDAS): Utilizing multiple GCIP products and partners in a continental distributed hydrological modeling system. *Journal of Geophysical Research: Atmospheres*, *109*, D07S90. https://doi.org/10.1029/2003JD003823

Nakagawa, M., Tanaka, K., Nakashizuka, T., Ohkubo, T., Kato, T., Maeda, T., … Ogino, K. (2000). Impact of severe drought associated with the 1997–1998 El Nino in a tropical forest in Sarawak. *Journal of Tropical Ecology*, *16*, 355–367.

Pagano, T., & Garen, D. (2005). A recent increase in western US streamflow variability and persistence. *Journal of Hydrometeorology*, *6*, 173–179.

Penman, H. L. (1948). Natural evaporation from open water, bare soil and grass. Proceedings of the Royal Society of London A: Mathematical, Physical and Engineering Sciences. The Royal Society, pp. 120–145.

Powell, E. J., & Keim, B. D. (2015). Trends in daily temperature and precipitation extremes for the Southeastern United States: 1948–2012. *Journal of Climate*, *28*, 1592–1612.

Qu, Y., & Duffy, C. J. (2007). A semidiscrete finite volume formulation for multiprocess watershed simulation. *Water Resources Research*, *43*.

Refsgaard, J. C., & Storm, B. (1996). *Construction, calibration and validation of hydrological models*. In *Distributed hydrological modelling* (pp. 41–54). Netherlands: Springer.

Saunders, M., Chandler, R., Merchant, C., & Roberts, F. (2000). Atlantic hurricanes and NW Pacific typhoons: ENSO spatial impacts on occurrence and landfall. *Geophysical Research Letters*, *27*, 1147–1150.

Seo, S., Sinha, T., Mahinthakumar, G., Sankarasubramanian, A., & Kumar, M. (2016). Identification of dominant source of errors in developing streamflow and groundwater projections under near-term climate change. *Journal of Geophysical Research: Atmospheres*, *121*(13), 7652–7672.

Soil Survey Staff (2013). N.R.C.S., United States Department of Agriculture. Web Soil Survey. Available online at http://websoilsurvey.nrcs.usda.gov/.

Souza Filho, F. A., & Lall, U. (2003). Seasonal to interannual ensemble streamflow forecasts for Ceara, Brazil: Applications of a multivariate, semiparametric algorithm. *Water Resources Research*, *39*(11), 1307. https://doi.org/10.1029/2002WR001373

Tramblay, Y., Bouvier, C., Martin, C., Didon-Lescot, J.-F., Todorovik, D., & Domergue, J.-M. (2010). Assessment of initial soil moisture conditions for event-based rainfall–runoff modelling. *Journal of Hydrology*, *387*, 176–187.

Van Genuchten, M. T. (1980). A closed-form equation for predicting the hydraulic conductivity of unsaturated soils. *Soil Science Society of America Journal*, *44*, 892–898.

Vogel, R. M., & Bolognese, R. A. (1995). Storage–reliability–resilience–yield relations for over-year water supply systems. *Water Resources Research*, *31*, 645–654.

Weaver, J. C. (2005). The drought of 1998–2002 in North Carolina—Precipitation and hydrologic conditions.

Webster, P. J., Holland, G. J., Curry, J. A., & Chang, H.-R. (2005). Changes in tropical cyclone number, duration, and intensity in a warming environment. *Science*, *309*, 1844–1846.

White, S. A., & Wang, Y. (2003). Utilizing DEMs derived from LIDAR data to analyze morphologic change in the North Carolina coastline. *Remote Sensing of Environment*, *85*, 39–47.

Wilhite, D. A. (1997). State actions to mitigate drought lessons learned. *Journal of the American Water Resources Association*, 961–968.

Wilhite, D. A., & Svoboda, M. D. (2000). Drought early warning systems in the context of drought preparedness and mitigation. Early warning systems for drought preparedness and drought management, 1–21.

Woldemeskel, F., Sharma, A., Sivakumar, B., & Mehrotra, R. (2012). An error estimation method for precipitation and temperature projections for future climates. *Journal of Geophysical Research: Atmospheres*, *117*, D22104. https://doi.org/10.1029/2012JD018062

Xia, Y., Mitchell, K., Ek, M., Sheffield, J., Cosgrove, B., Wood, E., … Meng, J. (2012). Continental-scale water and energy flux analysis and validation for the North American Land Data Assimilation System project phase 2 (NLDAS-2): 1. Intercomparison and application of model products. *Journal of Geophysical Research: Atmospheres (1984–2012)*, *117*, D03109. https://doi.org/10.1029/2011JD016048

Xie, P., & Arkin, P. A. (1997). Global precipitation: A 17-year monthly analysis based on gauge observations, satellite estimates, and numerical model outputs. *Bulletin of the American Meteorological Society*, *78*, 2539.

Yao, H., & Georgakakos, A. (2001). Assessment of Folsom Lake response to historical and potential future climate scenarios: 2. Reservoir management. *Journal of Hydrology*, *249*, 176–196.

Yu, X., Duffy, C., Baldwin, D. C., & Lin, H. (2014). The role of macropores and multi-resolution soil survey datasets for distributed surface–subsurface flow modeling. *Journal of Hydrology*, *516*, 97–106.

Zhao, G., Gao, H., Naz, B. S., Kao, S.-C., & Voisin, N. (2016). Integrating a reservoir regulation scheme into a spatially distributed hydrological model. *Advances in Water Resources*, *98*, 16–31.

SUPPORTING INFORMATION

Additional Supporting Information may be found online in the supporting information tab for this article.

How to cite this article: Zhang M, Chen X, Kumar M, Marani M, Goralczyk M. Hurricanes and tropical storms: A necessary evil to ensure water supply? *Hydrological Processes*. 2017;1–15. https://doi.org/10.1002/hyp.11371